STUDY OF HIGHLY ISOCHRONOUS BEAMLINES FOR FEL SEEDING

C. Sun, H. Nishimura, G. Penn, M. Reinsch, D. Robin, F. Sannibale, C. Steier, W. Wan#
Lawrence Berkeley National Laboratory (LBNL), Berkeley, CA 94720, USA

Abstract

Recently, seeding schemes such as echo-enabled harmonic generation (EEHG) for short (nm) wavelength FELs have been proposed. These schemes require that the nm-level longitudinal bunch structure be preserved over a distance of several meters. This is a challenge for the beamline design. In this paper we present our studies of several solutions for beamlines that are nearly isochronous.

INTRODUCTION

It is desirable to seed a soft x-ray FEL starting from a conventional laser source. The echo scheme [1], which utilizes two laser-electron interaction processes, each followed by a chicane, is a promising method to achieve this goal. A schematic of an EEHG beamline is shown in Fig. 1. The first two undulators are tuned for interactions with conventional laser sources, while the final undulator is tuned for a very high harmonic of these input lasers. The first chicane has an extremely large R56, leading to overbunching of the modulated beam and creating energy bands in phase space, as shown in Fig. 2(left). The second chicane yields a conventional phase rotation of the electron beam, transforming the energy bands into distinct microbunches, as shown in Fig. 2(right). When the beamline is properly tuned, the resulting current modulations contain significant harmonic content in a narrow band of wavelengths.

The echo scheme has the advantage of allowing for a very large harmonic jump in one stage, from optical to as low as ~1 nm, while introducing a modest increase in the energy spread of the electron bunch. This process has a very favorable dependence of generated bunching versus harmonic jump h at fixed energy modulation, scaling as $h^{-1/3}$. However, various effects may degrade this bunching factor. One particularly important effect is coupling between transverse motion and the time of flight across the echo beamline. Because different particles will have different transverse amplitudes, rapid variations in current will be smeared out due to the spread of transverse angles within the electron beam.

This effect is most deleterious in the region between the second and third undulators; here, the bands in phase space are closely spaced not only in energy but also in distance, on a length scale comparable to the target output wavelength. Before interacting with the second laser, regions having a high phase space density at a given energy are separated in longitudinal position by the much longer wavelength of the input laser.

*Work supported by the Director Office of Science of the U.S. Department of Energy under Contract No. DE-AC02-05CH11231.
#wwan@lbl.gov

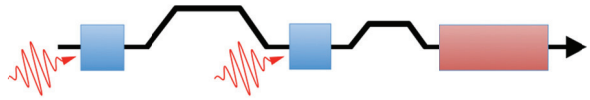

Figure 1: A schematic of an EEHG beamline.

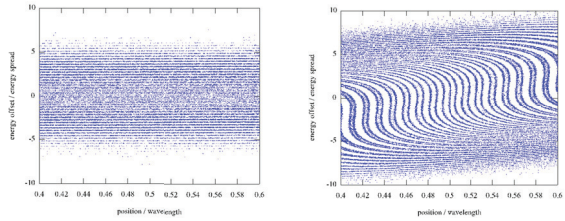

Figure 2: Phase space after first chicane (left) and after second chicane (right).

It is clear that to preserve the bunching at close to the ideal value, the spread in times of flight across the region from the second undulator to the third must be smaller than the target x-ray wavelength. In this paper, we calculate the spread in time of flight for three beamline designs of varying complexity. At the most basic level, the time of flight is given by nonlinear transport terms according to the following equation:

$$c\Delta t = T_{511}x^2 + T_{522}(x')^2 + T_{512}xx' + \{y\ \text{terms}\} + \cdots$$

Cross-terms and transport coefficients of higher order may also contribute. Here, the contribution from the R56 of the chicane is not included, as this is part of the idealized map which generates the short-wavelength bunching; neither is the T566 term, which represents a distortion rather than a smearing out of the longitudinal phase space. The key terms are proportional to the transverse amplitude, so this effect scales with the geometric emittance. The spread of Δt is the main concern here; for the simplified case where the initial Courant-Snyder parameter [2] α_x=0, all terms are uncoupled and add in quadrature, yielding

$$c^2\sigma_t^2 = \varepsilon_x^2\left(2T_{511}^2\beta_x^2 + T_{512}^2 + \frac{2}{\beta_x^2}T_{522}^2\right) + \{y\ \text{terms}\} + \cdots$$

There are many additional terms when $\alpha_x \neq 0$.

In the simplified case where all focusing is linear and there is no dispersion outside of the chicanes, the distribution function should be ellipsoidal in transverse phase space. The spread in time of flight can then be described as an integral of Courant-Snyder parameters for that section of beamline, according to

$$c^2\sigma_t^2 = (1+a_x^2)\left(\frac{\varepsilon_x}{2}\int_{z_1}^{z_2} dz\,\frac{1+\alpha_x^2}{\beta_x}\right)^2 + \{y\ \text{terms}\},$$

Where $0 < a_x < 1$ represents the variation from the initial betatron phase of each electron, and can be expressed as integrals of α, β, and the phase advance. Over a large phase advance > π/2, a_x will typically be small and transverse amplitude alone mostly determines the slippage. Because transverse angles scale as $(1+\alpha^2)/\beta$,

ISBN 978-3-95450-117-5

large values of α are just as deleterious as small β. Thus, any strong focusing element will tend to disrupt the bunching. This constraint is most significant for attosecond pulses where, to avoid lengthing of the pulse through slippage, the radiating undulator must be so short that there is no FEL gain. The peak power reaches a plateau at the value

$$P_{\text{atto}} \approx \frac{m_e c^3}{4 r_e \sigma_x \sigma_y}\left\{\frac{a_u}{\gamma}[J_0(\xi)-J_1(\xi)]b\frac{\ell\lambda_u}{\lambda}\frac{I}{I_A}\right\}^2,$$

Where σ_x, σ_y are the size of the electron beam, a_u is the undulator parameter, $\xi=a_u^2/2(1+a_u^2)$, ℓ is the length of the prebunched beam, I and b are the local current and bunching parameter, and $I_A=ec/r_e$ is the Alfvén current. The bunching is defined as $b=\left|\langle\exp(-2\pi i c t_p/\lambda)\rangle\right|$, where t_p is the time of flight. The power saturates after a distance $\ell\lambda_u/\lambda$, and for longer undulators the energy in the pulse will be roughly $P_{\text{atto}}L\lambda/c\lambda_u$, where L and λ_u are the undulator length and period. These expressions ignore evolution of the bunching, diffraction, and the hourglass effect. The number of photons produced scales as $b^2/(\beta_x\beta_y)^{-1/2}$. It is desirable to have small β in the last undulator, but not at the expense of reduced bunching. For a more typical FEL which amplifies the signal up to saturation, the initial value of the bunching and beta function are less significant, although bunching must remain well above noise levels. For a given beamline, transport to the x-ray undulator will degrade the ideal bunching, b_0, to a smaller value by a fixed multiplicative factor, which we will denote as b/b_0.

We consider parameters related to LBNL design studies for a soft x-ray FEL, with an electron energy of 1.8 GeV, peak current 500 A, normalized emittance 0.6 micron, and energy spread up to 500 keV after seeding. With undulators having a 20 mm period, photon pulses can be generated with photon energies ranging from 280 eV to 1 keV. At close to 1 nm length scale, even this low-emittance beam will suffer significant damping of the seeded bunching unless the lattice is carefully design to minimize the effect of coupling to transverse motion.

For the attosecond configuration, the seed lasers can have wavelengths down to 200 nm and interact in ~1 m long undulators having periods down to 200 mm. We consider three types of magnetic optics in between the second and third undulator: a simple drift beamline; a quadrupole lattice with simultaneous focusing in both planes; and an isochronous beamline using multiple bends and sextupole magnets, similar to those designed for the arcs of ERLs.

SIMPLE DRIFT AND QUAD BEAMLINES

First, a simple 7-meter drift beamline between the second and third undulator is studied. The waists of the horizontal and vertical beta functions are set at the center of the beamline, and equal to 6 meters (about 8 meters at the end of the beamline). The spread in times of flight across the beamline is calculated by tracking 1000 particles populated according to the beam condition above. The contribution terms are evaluated using Differential Algebra (DA) based tracking codes, such as COSY [3] and Goemon7 [4]. The results are shown in Table 1. This drift beamline has a reasonable value of the bunching factor, however with the expense of the photon scaling factor due to large beta functions at the second undulator.

To control beta functions of the beamline, 10 quadrupoles are introduced to the beamline. To have mirror symmetric optics functions, these 10 quadrupoles are mirror-symmetrically formed in 2 groups. Genetic algorithm is then applied to minimize both the time of flight spread and the beta function of this beamline. The optimization variables are quadrupole strengths, distance between quads, and endpoint beta functions. The optimization constraints are that the maximum beta functions are less than 30 meters, and the beta functions at the end of beamline are the same as the ones at the entrance to assure the symmetry. We also demand that the beta functions at both ends of the beamline are at their waists, i.e., $\alpha_x=\alpha_y=0$. The optimal solution front is shown in Fig. 3. A trade-off between the time of flight spread and beta function is clearly seen. To have a small spread solution, a large beta function is required, and vice versa. For the solution with beta function about 2.4 meters, the spread is about 0.8 nm as shown in the figure. The optics functions and magnetic layout of this lattice are shown in Fig. 4. The differential contribution terms of the spread are calculated using DA code, and results are shown in Table 1.

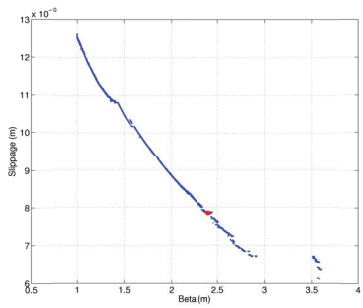

Figure 3: Solutions front for the optimized quadrupole beamline. The red dot indicates the lattice solution shown in Fig. 4.

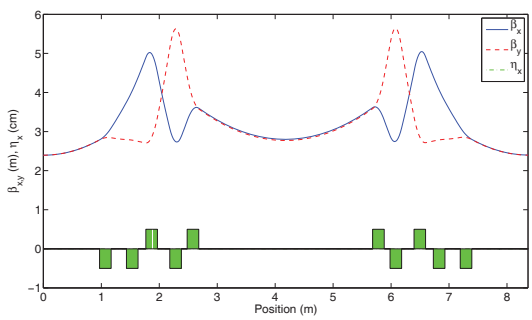

Figure 4: Optics functions and magnet layout of the quadrupole beamline.

AN ISOCHRONOUS BEAMLINE

Although the quadrupole beamline above has been optimized for a small spread of time of flight and beta

ISBN 978-3-95450-117-5

functions, the spread is still of the same order of the x-ray FEL wavelength (about nm), and the photon scaling factor $(b/b_0)^2/(\beta_x\beta_y)^{-1/2}$ is small. This reflects the difficulty in producing strong focusing, especially simultaneously in both planes, without generating large values of α. To preserve nm-level longitudinal bunch structure, however, we need to further reduce the time of flight spread. As shown in Table 1, the dominant contribution terms for the quadrupole beamline are T511, T522, T533, and T544. To correct these terms, several bends and sextupoles are introduced to the beamline. The magnet layout of this beamline is shown in Fig. 5. It has two mirror-symmetric cells, and each cell has another mirror-symmetric structure, consisting of two bend families (B1 and B2), three quadrupole (Q1, Q2 and Q3) and sextupoles (S1, S2 and S3) families.

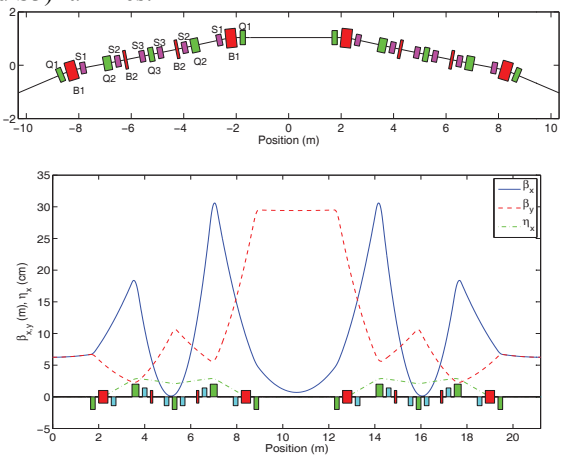

Figure 5: Magnet layout (top) and optics functions (bottom) for an isochronous beamline. To illustrate the bending of the beamline in the layout, the bending angles are scaled by 10 factors for all the bends.

The code COSY is applied to correct the dominant contribution terms by varying the quadrupole and sextupole strengths. An optimized lattice solution is shown in Fig. 5, and contribution terms are summarized in Table 1. We can see that after the correction, all the second order contribution terms are reduced to less than 1 pico-meter, and the remaining third order terms are around the pico-meter level. Thus, a nearly isochronous beamline design is achieved. For this beamline, the spread of time flight is about 5 pm, and the photon scaling factor is about 30 times larger than the one of the optimized quadrupole beamline.

The effects of fringe field, misalignment and multipole errors for this beamline have also been investigated, and their impacts on the spread of time flight can be neglected for reasonable values.

Figure 6 shows the longitudinal phase spaces of the electron beam before and after the isochronous beamline with a chicane (R56 = 180 μm) on. We can see that the fine structure of the longitudinal phase space is perfectly preserved.

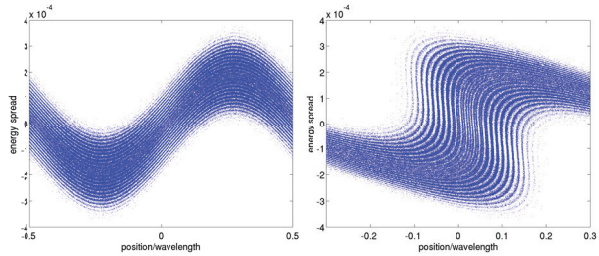

Figure 6: Phase space before (left) and after (right) the isochronous beamline with chicane on.

Table 1: Parameters for three different beamlines.

Lattice	Drift	Quad	Isochronous
[a]$\beta_{x,y}$ (m)	8.04	2.39	6.25
L (m)	7	8.3	21.2
[b]T511 (pm)	0	230	< 1
[b]T522 (pm)	74	273	< 1
[b]T533 (pm)	0	231	< 1
[b]T544 (pm)	74	354	< 1
[b]U5112 (pm)	0	< 1	2.62
[b]U5116 (pm)	0	< 1	4.24
[b]U5224 (pm)	0	< 1	1.13
Spread (pm)	146	780	5.2
Bunching $\lvert b/b_0\rvert$	0.790	0.106	0.999
$(b/b_0)^2/(\beta_x\beta_y)^{-1/2}$	0.078	0.0047	0.159

[a] β functions at the end of beamline.
[b]The electron beam sizes and angles have been included in these contribution terms.

CONCLUSIONS

In this paper we present three types of beamline design for echo-enabled harmonic generation (EEHG) FEL: a simple drift beamline which has a reasonable value of bunching factor, but a small photon scaling factor due to large beta functions; a pure quadrupole beamline which has beta functions control, but a small bunching factor; and a nearly isochronous beamline with both a large bunching and photon scaling factors. A pico-meter level of spread in times of flight has been achieved for the isochronous beamline. Further performance gains require a study in reducing the beta function produced by the isochronous beamline.

REFERENCES

[1] G. Stupakov, Phys. Rev. Lett. **102**, 074801 (2009).
[2] E.D. Courant and H.S. Snyder, Ann. Phys. **3** (1958) 1.
[3] K. Makino and M. Berz, Nucl. Instrum. Meth. Phys. A **427** (1999) 338.
[4] H. Nishimura, Proceedings of the 2001 PAC, Chicago, IL, USA, 3066 (2001).

ISBN 978-3-95450-117-5